

11th International Pyrotechnics Seminar, Vail, Colorado, 7-11 July 1986

INFRARED THERMOGRAPHIC STUDY OF LASER IGNITION

Jonathan H. Mohler
Monsanto Research Corporation
Mound*
Miamisburg, Ohio 45342

Charles T. S. Chow
Lawrence Livermore National Laboratory
P. O. Box 808
Livermore, California 94550

This document is
PUBLICLY RELEASABLE
Henry Keyes (OSTI)
Authorizing Official
Date: 7-6-09

ABSTRACT

Pyrotechnic ignition has been studied in the past by making a limited number of discrete temperature-time observations during ignition. Present-day infrared scanning techniques make it possible to record thermal profiles, during ignition, with high spacial and temporal resolution. Data thus obtained can be used with existing theory to characterize pyrotechnic materials and to develop more precise kinetic models of the ignition process.

Ignition has been studied theoretically and experimentally using various thermal methods. It has been shown that the whole process can, ideally, be divided into two stages. In the first stage, the sample pellet behaves like an inert body heated by an external heat source. The second stage is governed by the chemical reaction in the heated volume produced during the first stage. High speed thermographic recording of the temperature distribution in the test sample during laser ignition makes it possible to calculate the heat content at any instant. Thus, one can actually observe laser heating and the onset of self-sustained combustion in the pellet.

The experimental apparatus used to make these observations is described. The temperature distributions recorded are shown to be in good agreement with those predicted by heat transfer theory. Heat content values calculated from the observed temperature distributions are used to calculate thermal and kinetic parameters for several samples. These values are found to be in reasonable agreement with theory.

*Mound is operated by Monsanto Research Corporation for the U. S. Department of Energy under Contract No. DE-AC04-76DP00053.

INTRODUCTION

The ignitability of thermite and other heat powder products is an extremely important performance parameter. Simple measurement of the stimulus level required for a single sample configuration and set of firing conditions does not supply enough information to confidently predict how well the same material will ignite under different conditions. Previous studies of hot wire ignition of thermites [1] outlined a procedure for measuring minimum ignition energy, excluding all losses due to thermal conduction. This approach, while useful as a characterization tool, provides no information about heat flow away from the heat source nor about temperature distribution at ignition. This kind of information is required to properly characterize a material with respect to ignitability and to model the ignition process. The purpose of the current study is to develop the techniques required to record the temperature profile in a sample throughout ignition and to use these data to develop a useful model of the ignition process.

We have chosen to study ignition using a laser heat source and using infrared thermography to monitor the sample temperature during ignition. Video thermography records a complete infrared image every 30 ms in its standard mode, but an optional mode can be used which scans a single line every 125 μ s. Assuming that the laser beam used to ignite the sample is focused at the sample surface and that the sample pellet is homogeneous, the temperature distribution will be hemispherically symmetrical, and a single dimension is sufficient to record heat flow in the sample. The total heat content of the pellet can be calculated from the observed temperature distribution, $T(r)$, using:

$$Q = 2\pi\rho C_p \int_0^R T(r)r^2 dr \quad (1)$$

where ρ is density and C_p is heat capacity, r is the radial distance and R is the sample radius. Heat flow theory predicts that temperature distribution at time = t produced by a point heat source will be

$$T(r,t) = T_0 + q/4Kr \operatorname{erfc} [r/2\sqrt{\alpha t}] \quad (2)$$

where T_0 is the initial temperature, q is the heat input in cal/s, K is thermal conductivity in cal/cm deg s, α is thermal diffusivity in cm/s, and $\text{erfc}(x)$ is the conjugate error formation of x . If one considers the laser to be a heat source with heat flux, q , the surface temperature history at the center of a spot $r < a$ (heated spot size is πa^2) will be given by:

$$T(0,0,t) = T_0 + 2q\sqrt{at}/K [1/\sqrt{\pi} - I\text{erfc}(a/2\sqrt{at})] \quad (3)$$

where $I\text{erfc}(x)$ is the integral of the conjugate error function of x ($I\text{erfc}(x) = \int [1 - \text{erf}(x)]dx$). When $a/2\sqrt{at}$ is large or t is small, $I\text{erfc}[a/2\sqrt{at}] \rightarrow 0$ and the temperature at the center of the beam spot can be approximated by the following equation, using $x = K/\rho C_p$.

$$\Delta T_{\max} = (2q/\rho C_p \sqrt{\pi}) \sqrt{t/\alpha} \quad (4)$$

The thermal diffusivity, α , can be calculated from this relationship if q , P , and C_p are known. This relationship can be applied to a reactive sample only during the preheating phase of the ignition process, since the sample behaves like an inert material during this phase.

EXPERIMENTAL

A schematic diagram of the measurement system is shown in Figure 1. The ignition beam from the 60 W, CO_2 laser is focused by a 50-cm focal length, ZnSe lens and reflected onto a face of the cylindrical sample. A HeNe laser is used to align system components and to locate the sample. A beam splitter reflects a portion of the CO_2 laser beam to a detector to monitor beam power.

In order to avoid problems associated with unstable mode structure in the CO_2 laser beam, the IR scanner was located to view the edge of the sample. A 20-degree wedge is cut from the sample to permit observation of the sample center, adjacent to the focal point of the laser beam. In this way thermal flow along the axis of the test part is recorded. The recorded infrared intensity is digitized and converted to temperature. A gaussian function can be used to fit the experimentally observed temperature distribution, $T(r)$, with excellent precision. A symmetrical distribution is generated by mathematical reflection of the single-sided data recorded from the pellet edge view. An iterative, nonlinear regression analysis is used

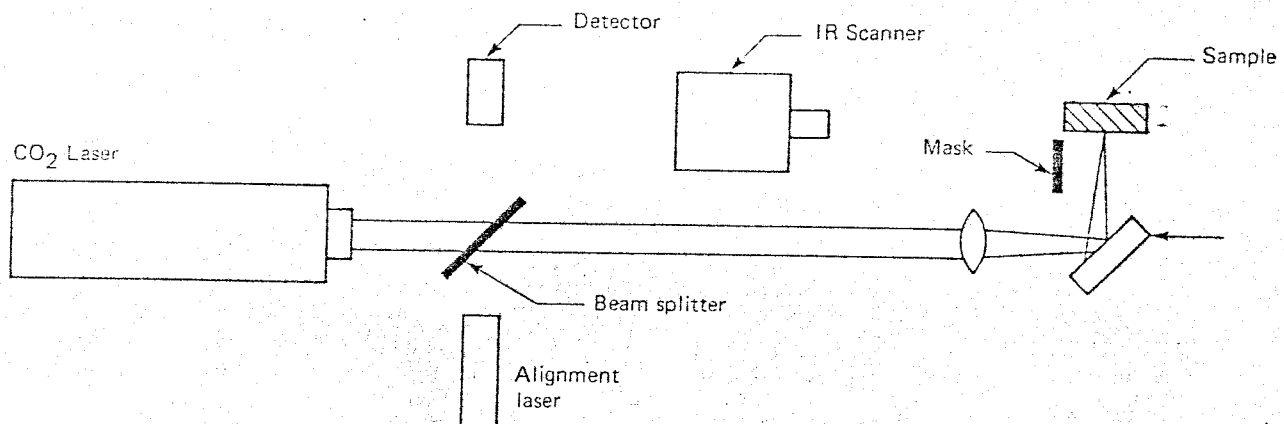


FIGURE 1 - Laser ignition system.

to find the best parameters for the gaussian function. The temperature data shown for three time segments in Figure 2 are typical of temperature distributions recorded and the precision achieved in fitting the gaussian function.

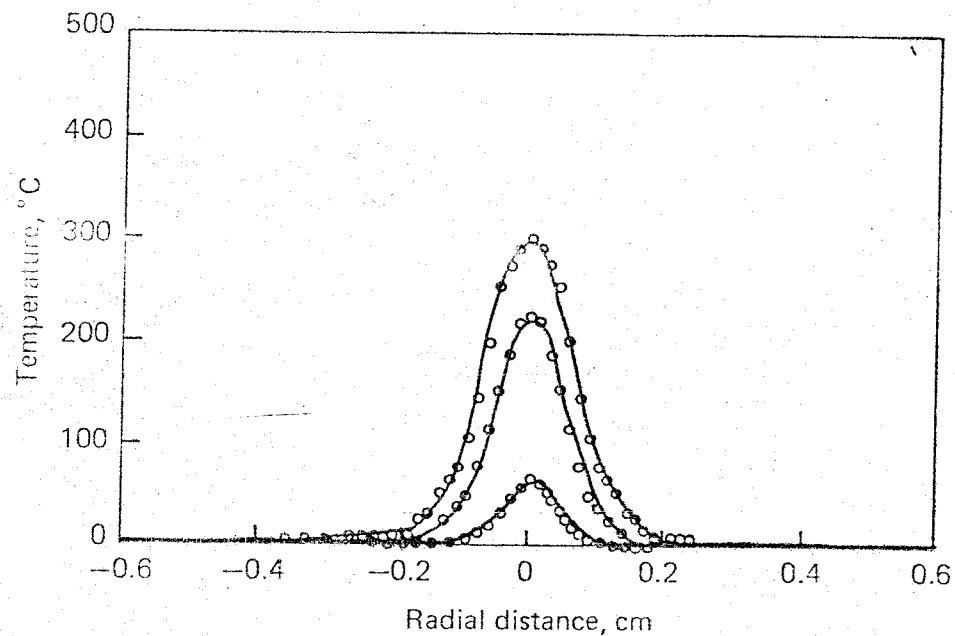


FIGURE 2 - Temperature distributions measured by thermographic scans at 41 ms, 75 ms, and 88 ms in test No. 167.

The fitted function becomes $T(r)$ in equation (1) for calculation of total heat, Q . The validity of the overall measurement and calculation procedure is illustrated by the data shown in Figures 3 and 4 for inert MACOR samples. The laser beam power measured prior to these measurements was 8 W, and the absorptivity observed for MACOR at 10.6 microns is 0.6. The expected heating rate should therefore be less than 4.8 W. The

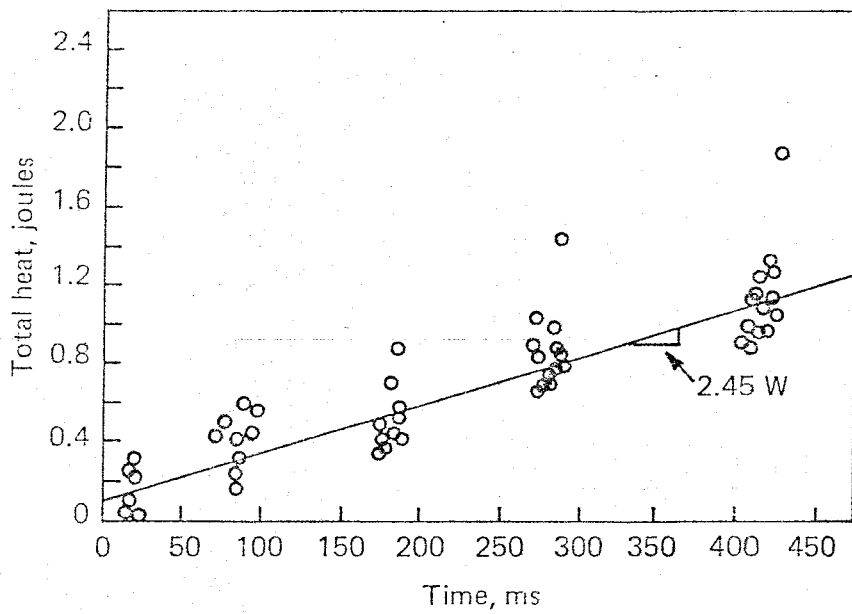


FIGURE 3 - Thermal rise in inert, laser-heated MACOR samples; laser power 8 W.

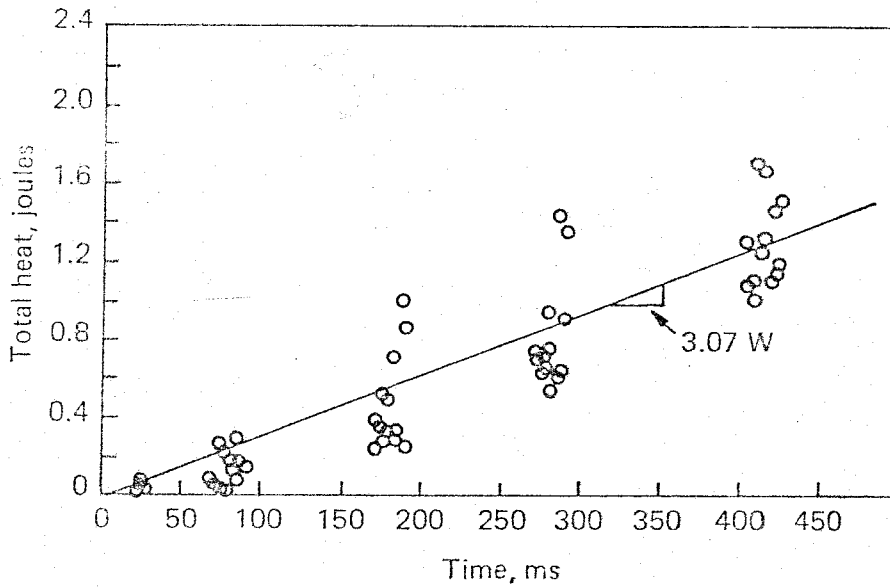


FIGURE 4 - Thermal rise in inert, laser-heated MACOR samples; laser power 8 W.

observed heating rates of 2.45 and 3.07 W are reasonable since other system and sample losses can account for the difference.

Samples were prepared by hot-pressing stoichiometric $\text{Fe}_3\text{O}_4/\text{Al}$ into cylindrical pellets, 1.9 cm diameter by 1.0 cm long, with a density of 2.0 g/cm³. Beam powers of 6, 8, and 10 W were used for ignition.

RESULTS AND DISCUSSION

The results of two runs which typify two different cases are plotted in Figures 5 and 6 as a ΔT_{\max} and Q, the integrated total heat, as a function of time. Run No. 167 represents the case where the surface is passivated by brief exposure to a subthreshold laser pulse, while a fresh surface was ignited in run No. 170. The curves that fit the data points in both Figures 5 and 6 are numerically generated in such a way that they share the same chemical-kinetic and thermal constants, such as E, the activation energy, and α , the thermal diffusivity of the thermite samples. The existence of two distinct regions can be seen during ignition in the temperature plots: a preheating region and a reaction delay region.

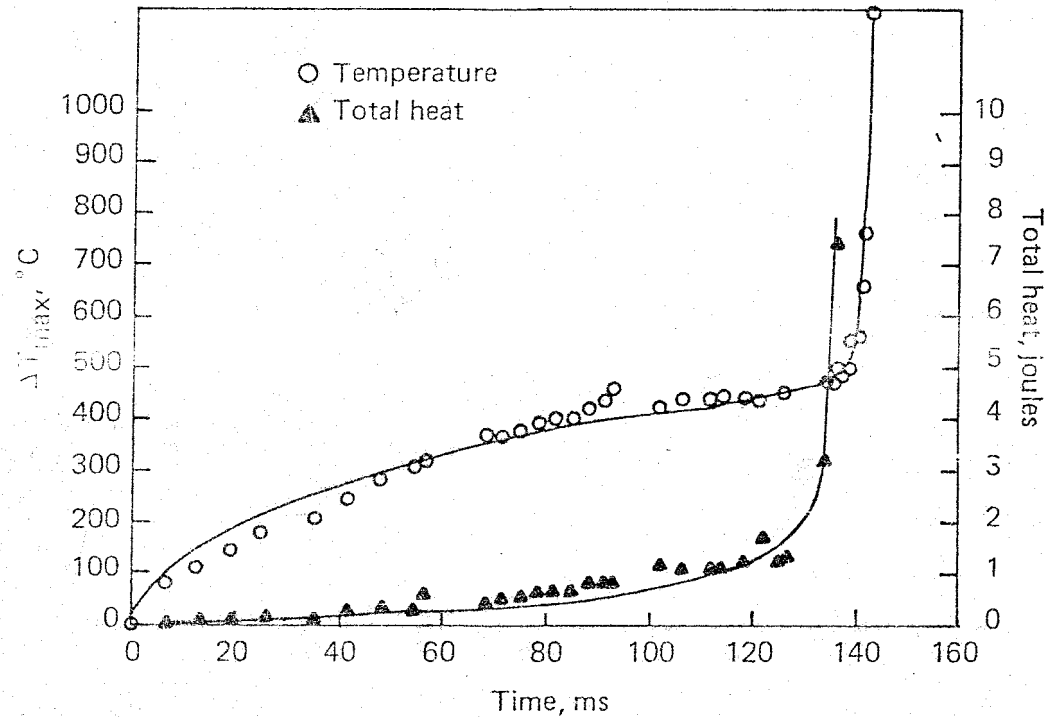


FIGURE 5 - Maximum temperature and total heat rise observed during laser ignition of $\text{Fe}_3\text{O}_4/\text{Al}$, run No. 167, 6-W laser power.

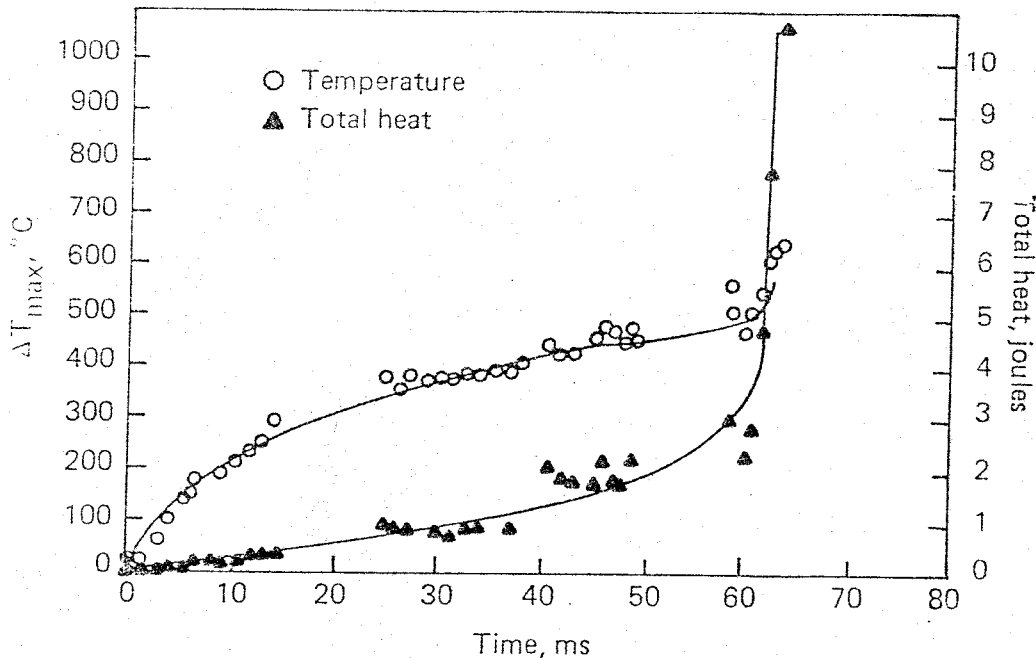


FIGURE 6 - Maximum temperature and total heat rise observed during laser ignition of $\text{Fe}_3\text{O}_4/\text{Al}$, run No. 170, 8-W laser power.

In the preheating region, the temperature history is correlated to the heating rate q by equation (4). In this same region, the slope of the Q versus t curve is proportional to q . In run No. 167 the 6 W laser power would be expected to produce a maximum heating rate of 4.2 W since the sample absorptivity was found to be 0.7. A heating rate of 4.2 joules/s, or 1 calorie/s, matches the apparent energy input rate in the preheating region. This suggests that only enough reaction energy to compensate for system and sample losses is being produced in the preheating region. Run No. 170, on the other hand, shows an apparent energy input rate of 6.6 cal/s, or 27.7 joules/s, which corresponds to about five times the maximum heating rate achievable by an 8-W beam. It is evident that this excess heating rate results from surface reaction induced by direct impingement on the laser beam.

Estimating a heated spot radius of 1 mm for the more ideally behaved run No. 167, an apparent energy flux, q , can be calculated. Using equation (4), the relative q value for run No. 170 can also be obtained. The results are summarized in the following table:

Run No.	Laser Power (W)	Apparent Energy Input Rate (cal/s)	Apparent Energy Input flux, q
167	6	1.0	32.0
170	8	6.6	51.0

These data allow us to extract two more pieces of information from the preheating portion of the ignition record. First, the apparent thermal diffusivity of the test samples is $2.0 \cdot 10^{-2}$ cm²/s. Second, the apparent heated spot size is approximately twice as large for the unpassivated sample surface tested in run No. 170 as that in run No. 167. This is consistent with the hypothesis that the difference between these runs results from flash surface reaction in run No. 170.

In the reaction delay region, the increasing slope of the Q as a function of t curve is a function of temperature according to the Arrhenius equation:

$$dQ/dt = Z e^{-E/RT} \quad (5)$$

where $T = T_{\max} + 298$ K. We assume that the reaction is zero order in the reaction delay region. Figure 7 shows a log plot of data points calculated by differentiating the fitted (Q as a function of t) curves in Figures 5 and 6 as a function of 1/T. The activation energy taken from the slope of this plot is -56 Kcal/mole.

Theory discussed by Merzhanov and Averson [2] indicates that ignition time should be related to energy flux in the following way:

$$t_{\text{ig}} \propto q^{-m}$$

with m less than 2.0. The following table summarizes the dependency of the total ignition delay time, t, on the apparent heat flux, q, for four ignition tests.

Laser Power (W)	Apparent Heat Flux (cal/cm ² -s)	$t_{\text{ig}} \cdot 10^{-3}$ (s)
6	32	142
8	51	64
10	56	43
10	99	33

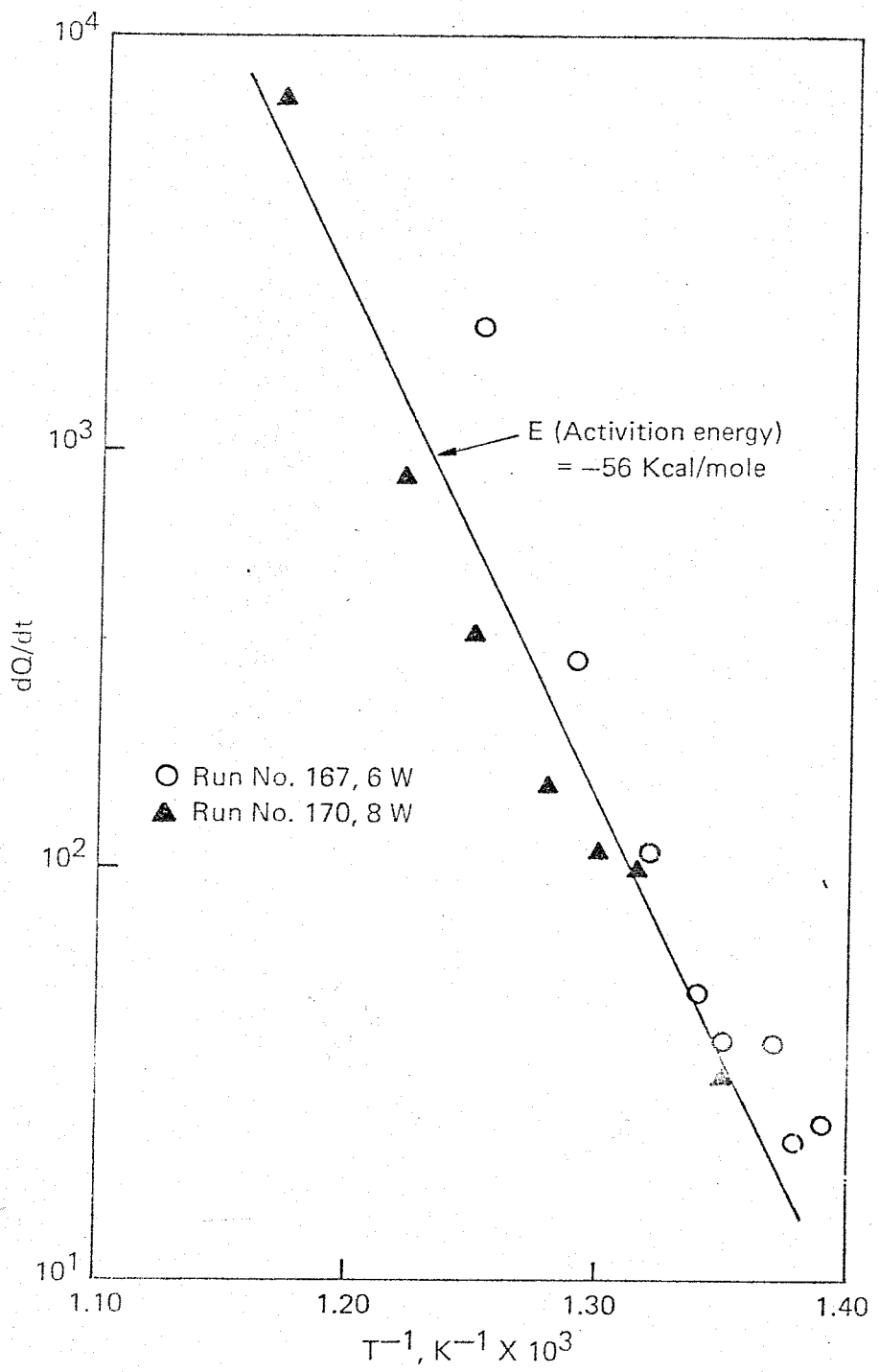


FIGURE 7 - Arrhenius plot of data taken from the temperature and heat curves shown in Figures 3 and 4 for run No. 167 and No. 170.

A log-log plot of these data, shown in Figure 8, indicates an m value of 1.40.

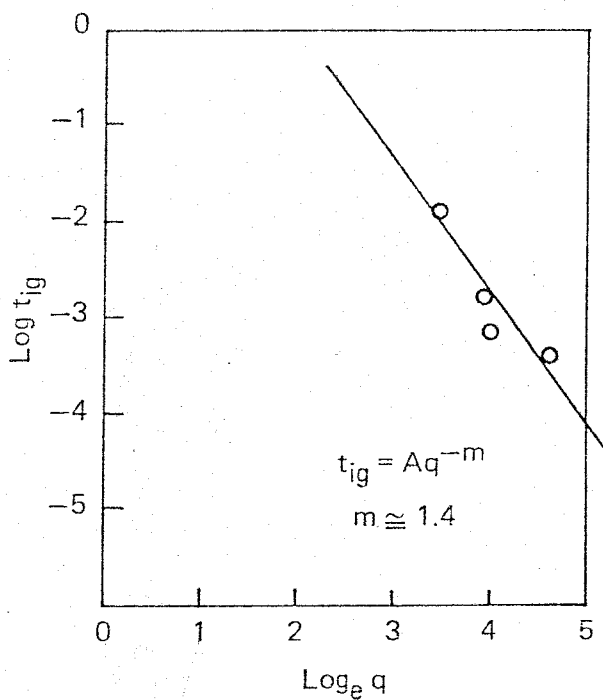


FIGURE 8 - Thermal flux - ignition time correlation.

Data taken for MACOR samples demonstrate the feasibility of extracting thermal diffusivity values from laser heating data for inert samples and reactive samples in the preheating region. The α value for MACOR is derived from a straight line fit of a plot of $T/[2q/\rho C_p \sqrt{\pi}]$ as a function of \sqrt{t} , shown in Figure 9, and is found to be $6.9 \cdot 10^{-3}$, which compares favorably with the published value of $6.0 \cdot 10^{-3}$ at 150°C .

CONCLUSIONS

Previous studies of pyrotechnic ignition have divided the ignition process into two stages [3-8], with the sample behaving essentially like an inert body during the early preheating stage, then reacting during the second stage in the heated volume produced by the preheating. A thermal discontinuity is caused at the surface of a laser ignited sample because of the high power density provided by a focused laser beam. This produces instantaneous, localized reaction at the point of beam impingement that is insufficient (at least in the case of thermites) to cause sustained

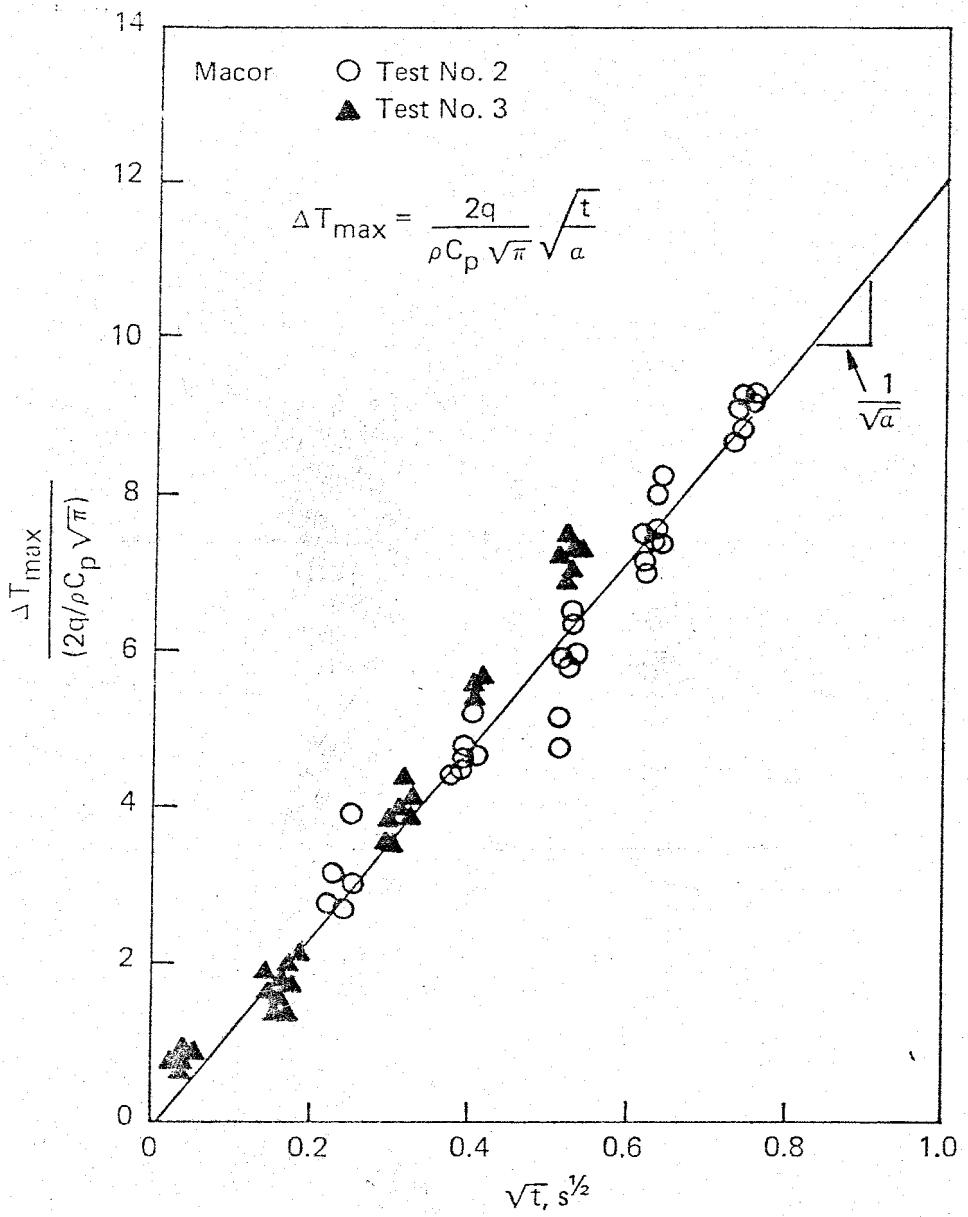


FIGURE 9 - Thermal diffusivity of MACOR derived from observed temperature and thermal flux data.

reaction. This limited surface reaction does, however, contribute significantly to the preheating stage of the ignition process. By using the apparent thermal flux observed in the preheating stage, we have been able to use classical ignition theory to analyze our data.

Run No. 167, in which a sample having a passivated surface was tested, was used mainly to illustrate the effect of surface reaction. However, it also suggests a possible technique for studying laser ignition by producing a small, inert, prereacted zone on the sample surface prior to ignition.

This work represents a beginning rather than a conclusion to our study of pyrotechnic ignition. A great deal needs to be improved to give better laser beam control, better thermographic standardization, and better data handling procedures, but we believe these results demonstrate the potential of our methods for studying the pyrotechnic ignition process.

REFERENCES

1. J. H. Mohler, "Power Independent Ignition Energy Measurements," presented at the 7th International Pyrotechnics Seminar, Vail, Colorado, July 14-18, 1980.
2. B. L. Hicke, Journal of Chemical Physics, 22:3, 414-429 (1954).
3. V. N. Vilyunov, Fizika Goreniya i Vzryva, 2:2, 77-82 (1966).
4. A. E. Averson, V. V. Barzykin, and A. G. Merzhanov, Fizika Goreniya i Vzryva, 4:1, 20-32 (1968).
5. V. I. Ermakov, A. G. Strumina, and V. V. Barzykin, Fizika Goreniya i Vzryva, 12:2, 211-217 (1976).
6. V. G. Abramov, V. T. Gontkovskaya, and A. G. Merzhanov, Izv. Kazan. Fil. Akad. SSSR, Ser. Khim., 5, 823-827 (1966).
7. A. G. Merzhanov and A. E. Averson, Combustion and Flame, 16, 89-124 (1971).
8. A. N. Gryadunov, A. P. Amosov, S. A. Bostandzhiyan, S. M. Muratov, and V. P. Filipenko, Fizika Goreniya i Vzryva, 18:4, 35-40 (1982).